ISSN: 2602-294X, Period: Triannual, Founded: 2016

NEURAL NETWORK ESTIMATION OF MUTUAL INDUCTANCE VARIATION FOR A SHADED-POLE INDUCTION MOTOR

Emre Çelik

Electrical and Electronics Engineering, Enginering Faculty, Duzce University, Düzce, Turkey.
*Corresponding Author: emrecelik@duzce.edu.tr

ABSTRACT

Shaded-pole induction motors (SPIMs) are often preferred in small power applications owing to their ability to work with single-phase power source, simple structure and low-cost properties. Such motors are within the class easy to manufacture, but the most difficult to analyze mathematically due to the fact that they have a variable air gap and elliptical rotating magnetic field, which leads to highly complex inductance calculations. Considering that the identification accuracy of phase variables is directly related to the correct knowledge of inductances in AC machines, the authors of this article attempt to realize a neural network (NN)-based inductance estimation in-between the stator and rotor, and also in-between the shading ring (shaded-pole winding) and rotor loop for an industrial SPIM. For this aim, corresponding inductance measurements are made first experimentally in terms of each 3.6º electrical position, and as such, a total of 101 data samples have been collected. %70 of them are considered as training data to train the NN while the remainder is adopted for testing the generation capability of NN. Results in comparison with the actual values have affirmed the excellence performance of the introduced NN in simultaneous estimation of the concerned two important inductances.

Keywords: Shaded-pole induction motors, shaded-pole, rotor loop, neural network, inductance estimation

1. INTRODUCTION

Shaded-pole induction motors (SPIMs) have a salient pole stator and a squirrel cage rotor. Although SPIMs have a simple structure in terms of manufacturing, the analysis of these machines is known to be quite hard owing to the elliptically rotating magnetic field generated in the machine air gap. There is no universally accepted technique for modelling this type of motor and implementing the motor performance analysis [1, 2]. The mutual inductances of SPIMs between stator and rotor loop, and also between shading ring and rotor loop are significant and exhibit a nonlinear variation depending upon the rotor angular position and motor phase current.

Artificial neural networks (ANNs) or neural networks (NNs) in short, are computing systems dedicated to mimic the essential behavior of biological neural system, which have seen much attention due to their capabilities in solving nonlinear problems by learning ability. They have some other unique properties such as excellent generalizing and learning capability from experience and examples, adaptation to changing situations, massive parallelism, and identification without exact knowledge. Via many nonlinear computational elements operating in parallel and connected to each other in between layers with intensive interconnections, NNs are able to accomplish the task of approximating the nonlinear behavior between input and

output data of a nonlinear model without prior knowledge about those data. They are very efficient and useful when the equations representing the respective model are nonlinear, complex, distributed in nature, and particularly vague or totally unknown with uncertain parameters [3]. As an alternative to neural network-based modelling, there are also studies adopting fuzzy logic for prediction of output parameters of a process according to its input parameters [4-8]. However, there are many parameters to be considered during the design of fuzzy logic system such as scaling factors, fuzzy-expert rules, membership functions etc. Determination of these parameters is still an ill-defined problem and based upon the experiences and knowledge of a skilled operator who gives several manual iterations over the considered system. Therefore, development of fuzzy-based prediction algorithm is tedious and time-consuming.

NNs have proved their remarkable contribution in a variety of applications, such as cover pattern recognition, control, diagnostic problems, fault detection, power electronics, forecasting, and function approximation. Since the topic of this paper is related to the estimation property of neural network, giving some introductory literature survey about this topic would be to the point. So far NN approach has been successfully employed in various estimation problems, such as estimating the output power and efficiency of a new-designed axial flux permanent magnet synchronous generator based on its rotational speed and the load connected to its terminals [3], online estimation for the rotor and stator resistances of an induction motor [9], predicting burr height produced in a sheet metal blanking process according to tool wear state and punch-die clearance [10], estimation of the distorted waveforms in power electronics [11], wind power generation estimation as a diagnostics tool [12], position estimation task in a speed sensorless switched reluctance motor drive system [13], finding the optimal tilt angle of PV panels in order to maximize the solar power from the sun [14], prediction of the nonlinear behavior of a newly designed wind energy harvester [15], and estimation of the clearance effect on blanking force, smooth sheared/fractured rate and burr height in the blanking process of CuZn30 sheet metal [16]. Nonetheless, the utilization of NN strategy to resolve the estimation concern of varying inductance parameters of a shaded-pole induction motor (CPIM) is currently open in the literature. That being said, this research paper may be considered as the first contribution of NN to estimate the challenging inductance values of a CPIM, which exhibit a nonlinear behavior in nature depending upon the angular position.

In the present paper, a total of 101 data samples including mutual inductance between stator and rotor (M_{ar}) and between shading ring and one rotor loop (M_{br}) have been collected from the experimental test bench with respect to the angular rotor position (θ) in steps of 3.6°. 70 samples of the observed data is used as the training data to train the developed network while the remaining samples are reserved for testing the generalization ability of previously trained network. For training, a well-known back propagation (BP) learning algorithm is employed. At the end of the study, outputs of the network, which are the predicted inductance values, are compared to their actual values for the test data, and the results have demonstrated that presented NN is able to establish a promising relationship among the outputs (M_{ar} and M_{br}) and the input variable of rotor position.

2. SHADED POLE INDUCTION MOTOR

Single-phase asynchronous motors are widely preferred for small power applications as they operate on single-phase grid with a robust and low-cost structure, which is manufactured easily and requires less maintenance. Their size increases at high powers, which degrades the ability

ISSN: 2602-294X, Period: Triannual, Founded: 2016

of these machines to compete with their three-phase counterparts owing to the increased cost [17]. They have an important advantage of being fed from a single-phase grid without need for a drive. Nonetheless, the inability to alter the direction of angular rotation, low starting torque along with low efficiency are among the main disadvantages of SPIMs with single shading ring [18-20]. The electrical and physical specifications of SPIM that we consider in this article are reported in Table 1.

Table 1. SPIM Parameters under consideration.

Parameter	Value	Parameter	Value
Nominal power, W	15	Rotor type	Squirrel cage
Nominal voltage, V	220	Rotor radius, mm	22
Nominal current, A	0.375	Slot number	26
Frequency, Hz	50	Stator winding number of turns	580
Pole number	4	Core depth, mm	25
Rotor speed, rpm	1305	Core size, mm	25×25

In AC machines, the identification accuracy of phase variables is directly related to the correct knowledge of inductances. Calculation of the inductances of SPIMs with variable air gap is quite difficult, and due to the variation of reluctance and saturation effect of the material used in the core, inductance in electric machinery is a nonlinear function of rotor position and phase current [21]. Inductance values in-between stator and rotor, and also in-between shading ring (shaded-pole winding) and rotor loop are acquired using a principle in [1], and they are used as the same in this article. In this sense, a lookup table that contains 101 data samples including the corresponding inductance values as output and rotor position as input is generated in which the sampling period of rotor position is 3.6°. In order to obtain the inductances at certain steps without disrupting the air gap, the test setup shown in Fig. 1 is established. In this setup, the SPIM is mechanically coupled to a PIC 16F877A controlled stepper motor which has a 1.8° step angle (200 steps/revolution). This means an electrical angle of 3.6° in SPIM.

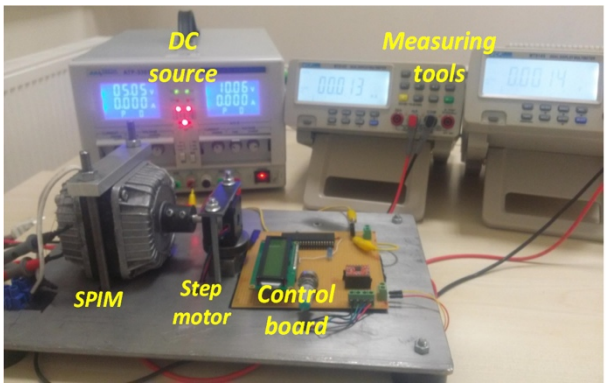

Figure 1. Test setup for the determination of mutual inductance.

The respective changes of stator-rotor loop mutual inductance (M_{ar}, mH) and shading ring-rotor loop mutual inductance (M_{br}, μH) as a function of angular rotor position are given in Fig. 2.

ISSN: 2602-294X, Period: Triannual, Founded: 2016

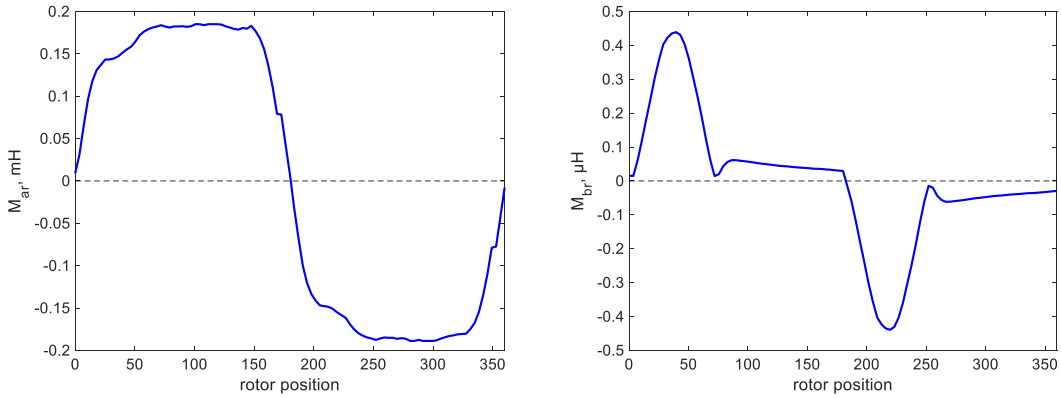

(a) **(b)**

Figure 2. Mutual inductance variation in a) stator-rotor loop b) shading ring-rotor loop.

3. THE DEVELOPED NEURAL NETWORK

One of the distinct characteristics of the NN is its ability to learn and generalize from experience and examples and to adapt to changing situations. NNs are able to map causal models (i.e. mapping from cause to effect for estimation and prediction) and inverse mapping (i.e. mapping from effect to possible cause). A NN is basically expressed by three kinds of parameters:

1. The interconnection pattern between different layers of nodes (or neurons, biologically)
2. The learning process for adjusting the weights of interconnections
3. The activation function that transforms a node's weighted input to its respective output

These parameters can be explained as follows: the connection weights connecting nodes in different layers each other influence the network performance crucially. Each node is usually connected with all of the previous and the next layer nodes. Modelling the relationship between the input and output patterns is realized by the training progress. Therefore, the input-output pattern matching is enabled when the network is trained successfully. The NN training progress essentially involves presenting a set of examples with known outputs and calculating error between the actual output pattern and the desired output pattern [10]. The connection weights are adjusted iteratively by an algorithm, i.e. BP algorithm until the presented input-output pattern matching is completed in a certain success in that the error falls below an acceptable value for the whole training sets. After the training is successfully finished, the generalization capability of the network is tested with examples that are not applied to the network before during training. A satisfactorily trained network is expected to be able not only to remember all the training examples, but to predict the required output adequately for an unseen input data which is onto the universe covered by the example patterns. Finally, the ability of a network to imitate nonlinear mapping property closely corresponds to the nonlinearity of the selected activation function. There are many types of transfer functions, such as threshold type, signum type or linear threshold type, or they can vary nonlinearly in a continuous form, such as sigmoid, inverse-tan, hyperbolic or Gaussian type. More particularly, user-defined activation functions can be declared for specific applications.

ISSN: 2602-294X, Period: Triannual, Founded: 2016

In our analysis, a three-layer network as illustrated in Fig. 3 is arranged with feedforward architecture which is the most widely use scheme today. The nodes of this network are indicated by the circles and the weights by the dots in the connections. The input variable is rotor position (θ, degree) while the quantities to be estimated from the input variable are selected as stator-rotor loop mutual inductance (M_{ar}, mH) and shading ring-rotor loop mutual inductance (M_{br}, μH), respectively. There are 18 neurons in the 1st hidden layer with hyperbolic tangent activation function, 11 neurons in the 2nd hidden layer with linear activation function which is also used for the output node. The input and output layers have nodes equal to the respective number of variables. Thus, such particular network can be defined as 1-18-11-2 network. There is not a systematic way for deciding the number of hidden layers, the number of nodes and the type of activation functions. They are usually selected in an arbitrary fashion depending on both the complexity of problem being solved and the desired accuracy. In this paper, we used the trial and error method by observing the network testing performance.

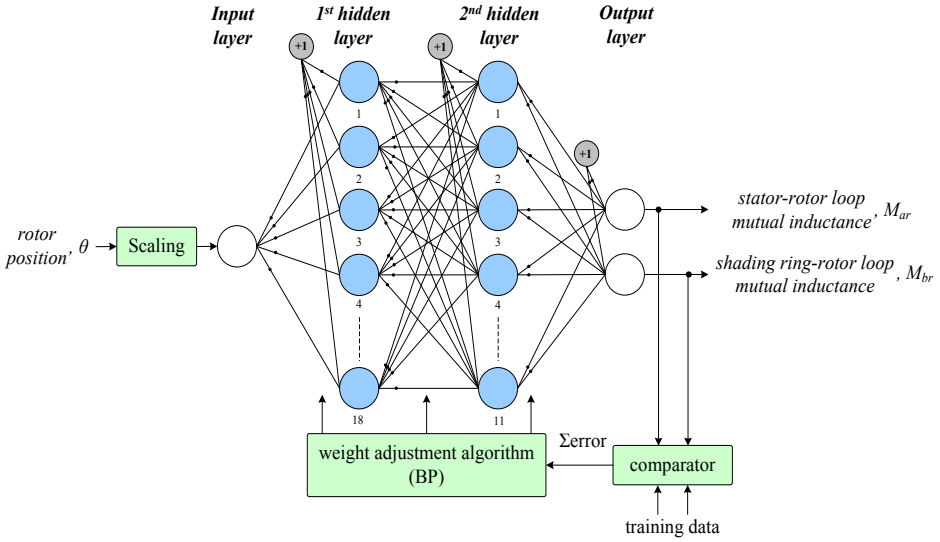

Figure 3. The developed 1-18-11-2 network configuration.

The aforementioned design is trained by employing BP algorithm. As the rotor position varies from 0° to 360°, which is a relatively greater range with respect to those of the NN output values, the range of the rotor position is transformed into the interval of [0, 1] prior to training process using Eq. 1. Such data normalization has proved to be useful and effective for the betterment of network estimation performance and also simplifying the computations significantly. In this equation, x_r and x_n are the actual and normalized value of a variable while x_{max} and x_{min} symbolize the maximum and minimum values of the respective variable.

$$x_n = \frac{x_r - x_{min}}{x_{max} - x_{min}} \quad (1)$$

As mentioned earlier, the total number of collected experimental data is 101, which is graphically visualized with regard to the rotor position in Fig. 2. The number of training samples that we use during training is 70 which are picked up homogenously from the whole experimental dataset, and the trained network is tested by the remaining 31 samples which are not used during training. For convenience, six of the training and test data are tabulated in Table 2.

Table 2. Twelve examples in the experimental dataset used for training and test purposes.

Dataset	θ (degree)	M_{ar} (mH)	M_{br} (μH)
Training set	0.0	0.009069	0.015221
	25.2	0.143319	0.357259
	100.8	0.185018	0.056588
	198.0	−0.133576	−0.241127
	277.2	−0.186357	−0.061289
	360.0	−0.007714	−0.029547
Test set	7.2	0.065789	0.060707
	64.8	0.181039	0.121772
	144.0	0.179756	0.039397
	237.6	−0.179861	−0.249365
	306.0	−0.186357	−0.044769
	342.0	−0.134794	−0.035367

Moreover, to provide a better picture concerning the training samples and test samples observed for M_{ar} and M_{br}, their evolution with respect to the rotor position is depicted in Fig. 4, where the training samples are specified by blue "○" marks and test samples by red "□" marks.

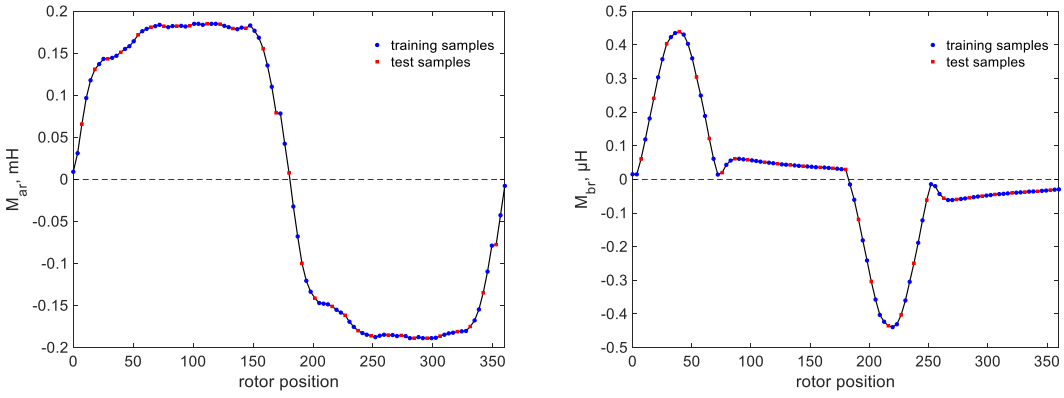

(a) **(b)**

Figure 4. Collected training and test samples for (a) M_{ar} (b) M_{br}.

4. INDUCTANCE ESTIMATION RESULTS AND PERFORMANCE ASSESSMENT

After the network is trained successfully, the network learning and generalizing capability of rotor position-inductance relations are checked for the case the test data includes unseen input rotor position values and the corresponding inductance values as output. To attain a well performed NN, we choose very small learning and momentum rates, and a very large number of training epochs which help the training error to converge gradually toward a minimal value in a stable trend. Fig. 5 shows the performance assessment criterion, namely, root mean-squared error (RMSE) for the training data as a function of iteration number. In line with what we desire, the RMSE drops from 0.6964 abruptly at first, then it approaches to a value of 0.01194 without any undesirable oscillation, signifying that the NN learns and gains the generalization property of rotor position-inductance relations as the training progresses. Also notice that after iteration 1×10^6, the error curve becomes almost stabile, and only very small amount of improvement is achieved after this point. If the training time is a concern and/or the results are satisfactory, the training process could be terminated here.

ISSN: 2602-294X, Period: Triannual, Founded: 2016

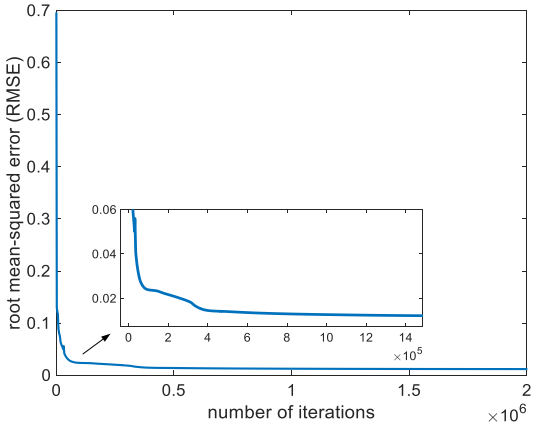

Figure 5. Root mean-squared error during training as a function of iteration number.

The experimental and the predicted values of stator-rotor loop mutual inductance by the designed NN model are shown in Fig. 6(a) in a superimposed manner for the test data. In addition, the percentage difference D_{MN} between the measured inductance L_M and the predicted inductance L_N by the NN model ($D_{MN} = (L_M - L_N)/ L_M$ %) is also given in Fig. 6(b) for each test sample. As seen from Fig. 6(a), there is a promising matching between the experimental results and the NN estimation. Except for the few cases, the percentage error rates are found to be very low. The mean error rate is calculated as 5.7% and it is to be noted that most of the error values favorably fall behind that mean error line.

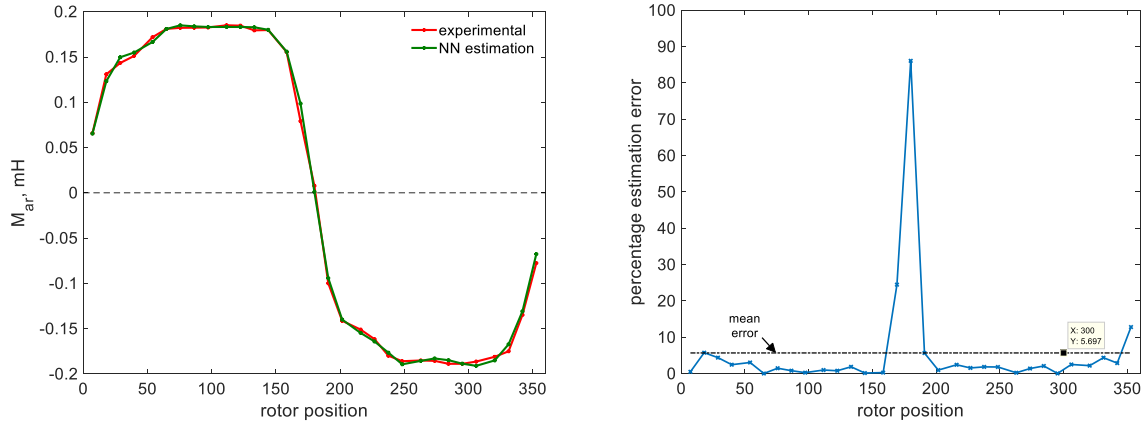

(a) **(b)**

Figure 6. Testing results for the estimation of M_{ar} (a) experimental and NN estimated M_{ar} variation (b) percentage error.

Finally, the NN estimation results regarding the shading ring-rotor loop mutual inductance along with the experimental observations are presented in Fig. 7(a), from which it is evident that the NN estimation curve is in good agreement with the experimental results. It is remarkable from Fig. 7(b) that the presented approach can estimate the shading ring-rotor loop mutual inductance value with a mean error rate of 14.7%. Similar to the previous case, many of the error values are far below the mean error line.

ISSN: 2602-294X, Period: Triannual, Founded: 2016

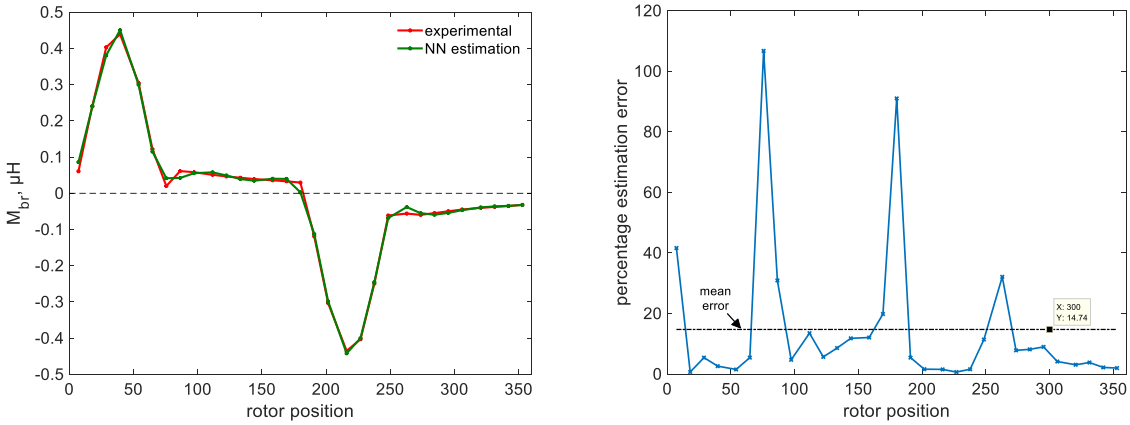

(a) **(b)**

Figure 7. Testing results for the estimation of M_{br} (a) experimental and NN estimated M_{br} variation (b) percentage error.

4. CONCLUSIONS

Due to the ability to work with single-phase power source, simple structure and low-cost properties, SPIMs are still in use today in small power applications. Since they have a variable air gap and elliptical rotating magnetic field, inductance calculations of such motors, which influence the identification accuracy of phase variables, are highly complex. For this reason, two important inductance parameters, such as stator-rotor loop mutual inductance (M_{ar}) and shading ring-rotor loop mutual inductance (M_{br}.) are estimated with respect to the angular position θ in this paper by the employment of NN strategy. A three-layer feedforward NN is designed in which rotor position is the input while the respective outputs are M_{ar} and M_{br}. Based on the real data collected from the experimental setup, the presented NN is trained by BP algorithm on a forward manner, which has produced satisfactory training results. Obtained results affirm the reliability and excellence of the proposed neural modeling in predicting the experimental test results with mean error rates less than 15%. Increasing the number of sampling data and iteration number can improve the results further. Moreover, more nodes can be included in the hidden layers and other activation function can be tried out in lieu of hyperbolic tangent and linear activation function.

Author Note: This research work was presented as an oral paper at the 3rd International Energy & Engineering Congress (UEMK2018).

REFERENCES

[1] Dalcalı, A. (2017). Gölge kutuplu asenkron motorların yeni bir matematiksel modeli ve uzay harmonikli eşdeğer devresi, Doktora tezi, Karabük Üniversitesi, Karabük.

[2] Dalcalı A, Akbaba A. Detection of the space harmonics of the shaded pole induction motor. Journal of Engineering Research 2017; 5: 95-105.

[3] Çelik E, Gör H, Öztürk N, Kurt E. Application of artificial neural network to estimate power generation and efficiency of a new axial flux permanent magnet synchronous generator. International Journal of Hydrogen Energy 2017; 42: 17692-17699.

[4] Wang K, Gelgele H, Wang Y, Yuan Q, Fang M. A hybrid intelligent method for modelling the EDM process. International Journal of Machine Tools and Manufacture 2003; 43: 995-999.

[5] Shabgard MR, Badamchizadeh MA, Ranjbary G, Amini K. Fuzzy approach to select machining parameters in electrical discharge machining (EDM) and ultrasonic-assisted EDM processes. Journal of Manufacturing Systems 2012; 32: 32-39.

[6] Simoes MG, Bose BK. Application of fuzzy logic in the estimation of power electronic waveforms. In: IEEE Industry Applications Conference Twenty-Eighth IAS Annual Meeting; 2-8 Oct. 1993; Toronto, Ontario, Canada. pp. 853-861.

[7] Yilmaz O, Eyercioglu O, Gindy NZ. A user-friendly fuzzy-based system for the selection of electro discharge machining process parameters. Journal of Materials Processing Technology 2006; 172: 363-371.

[8] Rodic D, Gostimirovic M, Kovac P, Radovanovic M, Savkovic B. Comparison of fuzzy logic and neural network for modelling surface roughness in EDM. International Journal of Recent advances in Mechanical Engineering 2014; 3: 69-78.

[9] Karanayil B, Rahman MF, Grantham C. Online stator and rotor resistance estimation scheme using artificial neural networks for vector controlled speed sensorless induction motor drive. IEEE Transactions on Industrial Electronics 2007; 54: 167-176.

[10] Hambli R. Prediction of burr height formation in blanking processes using neural network. International Journal of Mechanical Sciences 2002; 44: 2089-2102.

[11] Kim MH, Simoes MG, Bose BK. Neural network based estimation of power electronic waves. In: 21st Annual Conference on IEEE Industrial Electronics; 6-10 Nov. 1995; Orlando, FL, USA. pp. 353-358.

[12] Li S, Wunsch DC, O'Hair EA, Giesselmann MG. Using neural networks to estimate wind turbine power generation. IEEE Transactions on Energy Conversion 2001; 16: 276-282.

[13] Paulson F, Prabhu VV. Back propagation based ANN technique for rotor position estimation of 8/6 switched reluctance motor. In: International Conference on Innovations in Information, Embedded and Communication Systems; 19-20 March 2015; Coimbatore, India. pp. 1-5.

[14] Chatterjee A, Keyhani A. Neural network estimation of microgrid maximum solar power. IEEE Transactions on Smart Grid 2012; 3: 1860-1866.

[15] Çelik E, Uzun Y, Kurt E, Öztürk N, Topaloğlu N. A neural network design for the estimation of nonlinear behavior of a magnetically-excited piezoelectric harvester. Journal of Electronic Materials 2018; 47: 4412-4420.

[16] Çelik E, Çavuşoğlu O, Gürün H, Öztürk N. Estimation of the clearance effect in the blanking process of CuZn30 sheet metal using neural network−A comparative study. International Journal of Informatics Technologies 2018; 11: 187-193.

[17] Saygın A, Ocak C, Dalcalı A, Çelik E. Optimum rotor design of small PM BLDC motor based on high efficiency criteria. ARPN Journal of Engineering and Applied Sciences 2015; 10: 9127-9132.

[18] Parasiliti F, Villani M, Castello M. PM brushless DC motor with exterior rotor for high efficiency household appliances. In: International Conference on Electrical Machines; 2-5 Sept. 2014; Berlin, Germany. pp. 623-628.

[19] Gao Y, Chau KT, Ye S. A novel chaotic-speed single-phase induction motor drive for cooling fans. In: Fortieth IAS Annual Meeting; 2-6 Oct. 2005; Hong Kong, China. pp. 1337-1341.

[20] Dalcalı A, Akbaba M. Comparison of the performance of bridge and bridgeless shaded pole induction motor using FEM. International Journal of Applied Electromagnetics and Mechanics 2017; 54: 341-350.

[21] Akcayol MA. Anahtarlamalı relüktans motorun endüktans değişiminin sinirsel-bulanık modellenmesi. Politeknik Dergisi 2002; 5: 287-292.